ADVANCED MATERIALS TECHNOLOGIES
www.advmattechnol.de

A Soft Touch: Wearable Tactile Display of Softness Made of Electroactive Elastomers

*Gabriele Frediani, Hugh Boys, Michele Ghilardi, Stefan Poslad, James J. C. Busfield, and Federico Carpi**

Fingertip-mounted tactile displays of softness are needed for various virtual- or augmented-reality applications such as surgical simulation, tele-operation, computer-aided design, 3D model exploration, and tele-presence. Displaying a virtual softness on a fingertip requires the generation of quasi-static large displacements at moderate forces (as opposed to high-frequency small vibrations at high forces), via a deformable surface, to control both the contact area and the indentation depth of the skin. State-of-the-art actuation technologies are unable to combine simple structure, low weight, and low size, as well as energy efficiency and silent operation. Here, the progress on the development of a non-vibratory display of softness made of electroactive polymers is reported. It consists of a hydrostatically coupled dielectric elastomer actuator, shaped as a bubble interfaced to the fingertip, having a weight of 6 g. Prototypes can generate displacements up to 3.5 mm and forces up to 1 N. By combining this technology with a compact hand tracking sensor, a simple and cost-effective virtual-reality system is demonstrated. A psychophysical study engaging 15 volunteers in poke and pinch tactile tasks shows that users can properly distinguish between different stimuli rendered by the display, with an accuracy correlated to the perceptual difficulty of the tactile comparative task.

1. Introduction

The development of a diversity of virtual- or augmented-reality systems is currently challenged by the lack of suitable actuation technologies for fingertip-mounted devices that can mechanically stimulate finger pads to render the softness of a virtual object. Possible applications include surgical simulators to train in the palpation of soft tissues,[1] hand-held interfaces for either tele-operation,[2] computer-aided design[3] or 3D model explorations,[4] as well as tele-presence systems to augment virtual social interactions with the missing sense of touch.[5]

In order to physically mimic the softness of a virtual object with a fingertip-mounted device, it is necessary to produce a tactual feeling as close as possible to that arising from the indentation of a real soft object with the fingertip. According to Srinivasan and LaMotte, for the perception of the softness of objects having a deformable surface, it is sufficient that our brain receives a purely tactile feedback, as opposed to a purely kinaesthetic feedback.[6] This is supported by evidence that an adequate perceptual response is achieved by ensuring a modulation of the contact area between the fingertip and the object.[7–9] Indeed, the change in contact area has been proposed as a new proprioceptive cue.[10]

Furthermore, it has recently been shown that, in addition to the contact area, the indentation depth is also an essential tactile stimulus and these two stimuli independently contribute to the perception of softness.[11] Therefore, controlling only the contact area, or only the indentation depth, is expected to be less effective than controlling both of them at the same time.[11]

This implies that effective renderings of softness cannot be obtained using the variety of wearable tactile displays that indent fingertips via stiff surfaces, which are however very useful for force feedback, especially to render shapes.[12–17] Indeed, as discussed by Srinivasan and LaMotte, when a fingertip is interfaced to a rigid surface, the pressure distribution over the fingertip and the related deformation of the skin (and therefore also the contact area) are independent of the interface's compliance; this means that the arising tactile stimuli do not adequately encode information on compliance.[6]

Such evidence implies that, in order to mimic the softness of a virtual object with fingertip-mounted devices, the most effective approach is to use tactile displays that can generate quasi-static (non-vibratory) forces, via a soft interface (deformable surface), so as to control both the contact area and the indentation depth.

Dr. G. Frediani, Prof. F. Carpi
University of Florence
Department of Industrial Engineering
Via di S. Marta, Florence 3 – 50139, Italy
E-mail: federico.carpi@unifi.it
Dr. H. Boys, Dr. S. Poslad
Queen Mary University of London
School of Electronic Engineering and Computer Science
Mile End Road, London E1 4NS, UK
Dr. M. Ghilardi, Prof. J. J. C. Busfield
Queen Mary University of London
School of Engineering & Materials Science
Mile End Road, London E1 4NS, UK
The ORCID identification number(s) for the author(s) of this article can be found under https://doi.org/10.1002/admt.202100016.

DOI: 10.1002/admt.202100016

Moreover, ideally, such devices should be sufficiently small and light-weight to be comfortably and unobtrusively arranged on fingertips,[18] so as not to impair the motion of the fingers during virtual-reality tasks. Similarly, such devices should not generate acoustic noise and heat, for the sake of comfort.

The combination of all these requirements is hard to meet with conventional actuation technologies. So, it should not be surprising that tactile feedback is still underutilized in wearable devices to mimic realistic interactions with soft bodies. Indeed, very few technologies have been described so far to meet these requirements. One of them is based on pneumatic actuation, typically used in three ways: i) tiny air jets produced by arrays of nozzles, which however limit the realism of the tactual feeling, as a soft interface is missing;[19,20] ii) pneumatically displaced rigid pins,[21] whose stiff interface however makes them more suitable for shape rather than softness renderings, as discussed above; and iii) inflated chambers, whose performance is typically limited by the need for bulky and noisy external instrumentation,[22–24] although attempts to reduce size and weight are ongoing.[25]

A different approach uses electrical motors that move flexible/stretchable structures, such as polymer membranes or fabrics, in contact with the fingertip; such mechanisms, however, typically lead to complex, bulky, and heavy displays.[26,27]

Another strategy employs electrostatic actuators, consisting of air-filled[28] or liquid-filled[29,30] chambers, sealed by an elastomeric membrane that is displaced by a pressurization of the internal air or liquid; the pressurization is induced by an electrostatic attraction between a fixed rigid electrode and another electrode that covers a flexible or stretchable substrate.[28–30] This actuation strategy, which so far has been demonstrated for miniature (up to a few millimeters) tactile interfaces with displacements lower than 1 mm, might be challenged for higher displacements by the need for a larger lateral size, due to the zipping effect required for pressurization.[29,30]

Such a lack of simple and affordable enabling technologies is currently preventing the transition of a range of applications of displays of softness to real-life systems. Here, we report on latest developments of a tactile display technology consisting of electroactive elastomers.

2. Dielectric Elastomer Actuation for Tactile Displays

The electromechanical transduction technology used in this work is based on dielectric elastomer actuators (DEAs).[31–33] They are part of the broader family of smart materials known as electromechanically active polymers,[34] as a change of size/shape can be achieved through the application of a voltage. The most basic DEA configuration consists of a thin membrane of an elastomeric dielectric material with compliant electrodes on its surfaces. When an electric field is applied across the dielectric material, the resulting electrostatic stress causes a compression perpendicularly to the electrodes and a concomitant expansion of their surfaces. The effective compressive stress, p, is described by the following equation.[33]

$$p = \varepsilon_r \varepsilon_0 E^2 = \varepsilon_r \varepsilon_0 \left(\frac{V}{d}\right)^2 \quad (1)$$

where ε_0 is the dielectric permittivity of vacuum, ε_r is the elastomer's relative dielectric constant, E is the electric field, V is the voltage, and d is the membrane's thickness. Due to the high electric fields needed to drive DEAs (≈10–100 V μm^{-1}), typical voltages required for 10–100 μm-thick membranes are within the kilovolts range.[31–33] DEAs are generally characterized by large electrical strains, fast and acoustically silent operation, compact size, low specific weight, shock tolerance, low power consumption, and no overheating.[31–33,35]

To date, there have been several reports on DEA-based tactile devices, for various needs, including vibratory interfaces,[36,37] vertical displacements of a rigid pin, either mono-directionally[38] or bidirectionally,[39] latero-tactile stimulation of the skin via arrays of pins,[40] as well as variable texturing of surfaces.[41–43] However, only two configurations have proved useful so far to obtain non-vibratory wearable tactile devices that can electrically change both the contact area and the indentation depth on a fingertip, and therefore can serve to display a virtual softness, as discussed above. The first configuration is represented by buckling DEAs, consisting of membranes that can protrude upon electrical driving, so as to stimulate the fingertip;[44,45] a buckling membrane design is nevertheless typically limited by relatively small amplitudes of the achievable vertical displacements and forces.[44,45] The second configuration is represented by hydrostatically coupled DEAs (HC-DEAs),[46] where in general an active (i.e., electroded) membrane is coupled via an insulating fluid to a passive membrane; in comparison to a single buckling membrane, HC-DEAs can enable tactile displays with improved electro–mechanical performance and electrical safety.[47,48] The HC-DEA technology was also used in this work, as presented below.

3. Structure and Working Principle of the Tactile Display

The whole structure of the display coincides with that of a particular kind of HC-DEA, shaped as an electrically deformable 'bubble,' as shown in **Figure 1**a. An active membrane, made of one or more elastomeric layers coated with compliant electrodes, acts as a DEA, which transfers actuation to a passive membrane, via an insulating fluid. The arrangement of the display ensures that the fingertip is maintained at a constant distance from the device, in contact with the passive membrane.

By modulating the voltage applied to the active membrane, both the indentation and the contact area of the skin can be varied. In particular, as any applied voltage causes the active membrane to increase its curvature, the maximum values of the contact area and indentation occur when the voltage is off, whilst they get to zero at the maximum voltage (Figure 1a). This configuration allows for an effective transmission of actuation from the active membrane to the fingertip, avoiding any direct contact between them. This feature provides not only electrical safety, but also avoids distortions of the active membrane by the fingertip, taking advantage from a redistribution of the internal fluid when the passive membrane is loaded by the finger. This is important to ensure that the thickness of the active membrane does not undergo local distortions, which might lead to premature dielectric breakdown.

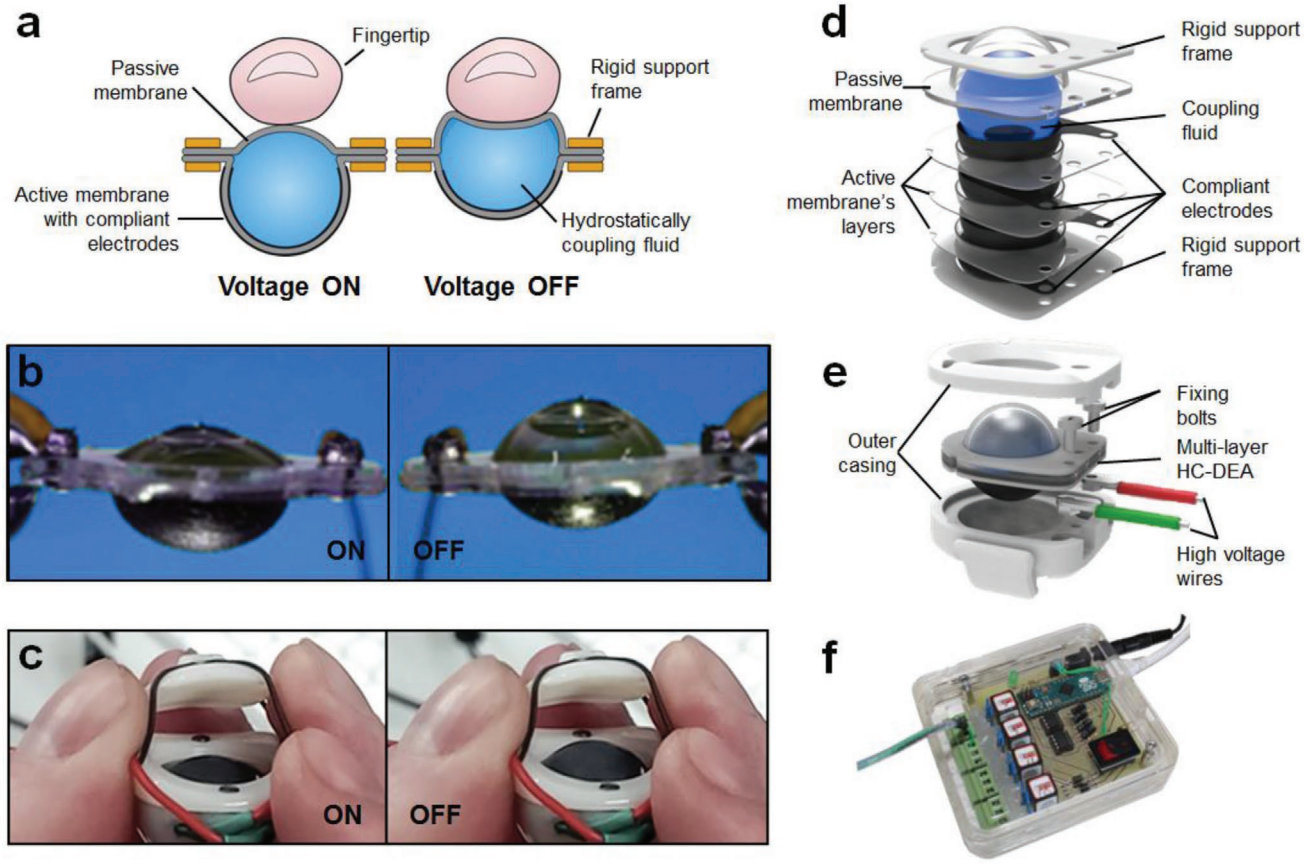

Figure 1. a) Schematic illustration of the structure of the tactile display and its working principle; for simplicity, the active membrane is represented with only one layer. b) Photos of an actuation of an HC-DEA sample. c) Photos of a prototype implementation of the tactile display in operation; note that, in that version, the finger was supposed to be secured also with a counter-frame above it, which however was not used in other versions of the display shown in this paper. d) Exploded rendering of an HC-DEA with a triple-layer structuring of the active membrane; the identical triple-layering (without electrodes) of the passive membrane is not shown for simplicity. e) Exploded rendering of the HC-DEA casing, to obtain the tactile display. f) Custom-made control electronics box, suitable to drive up to four tactile displays, independently.

Figure 1b,c shows prototype samples of the device. Following an initial presentation of this type of device[47] and later developments,[49,50] here we describe an improved design, which allowed for: i) increasing the output force; ii) reducing the device size, so as to facilitate multifinger systems; iii) integrating it with a commercial hand tracking sensor, so as to demonstrate a simple virtual-reality system for visuo–tactile interactions with computer-generated soft bodies; and iv) demonstrating the efficacy of the whole system with a psychophysical study, which involved 15 participants.

4. Results and Discussion

4.1. Tactile Display Design and Fabrication

In order to increase the force output, the active membrane of the HC-DEA bubble was designed with a multilayer structure, consisting of several dielectric elastomer layers intertwined with compliant electrode layers. This combination of multiple layers resulted in a stack (mechanical series) of elastomeric capacitors, which were electrically connected in parallel. This made the active membrane thicker (and therefore also stiffer), thereby ensuring a higher blocking force, without increasing the driving voltage. The increased force was also due to an increased thickness of the passive membrane too, which was made identical to that of the active membrane, by stacking an equal number of layers (without electrodes), so as to maintain the device symmetry (see the Experimental Section).

Different versions of the actuator, with membranes consisting of one, two, three, or four layers, were manufactured for performance comparisons. As an example, a sample with a triple-layer structure is schematically shown in Figure 1d. The employed materials and manufacturing processes are detailed in the Experimental Section. Following the assembly, the final shape of both the passive and active membranes of the HC-DEA bubble was a spherical cap, having a height of 5.5 mm and a base diameter of 12.5 mm. That size was empirically defined as a (non-optimized) trade-off between the need for maximizing the contact area with the fingertip (so as to maximize the perceptible force) and the need for minimizing the overall encumbrance of the device.

The HC-DEA bubble was fitted in a plastic casing, shown in Figure 1e. The casing's shape allowed the finger pulp to rest

in contact with the passive membrane. In addition to comfortably securing the device to the fingertip, the casing was also conceived to be as compact and light as possible, so as not to burden the user.

Furthermore, the design of the casing's shape, size, and surface finishing were affected by the intention to use the tactile displays in combination with an off-the-shelf and low-cost optical hand tracking sensor, so as to continuously detect the spatial position and orientation of the fingers. The possibility to combine the two technologies was considered of primary importance, in order to easily obtain an affordable virtual-reality system. The selected sensing technology was the LEAP Motion hand tracking system.[51] It uses stereo infrared cameras to track motions, without markers. While other optical systems are also available, such as Kinect (Microsoft, USA) and Duo MLX (Code laboratories, USA), we opted for LEAP Motion, as we focused on interactions with virtual objects at a desktop scale, where that sensor competitively offers high accuracy at a low cost. In particular, the LEAP Motion system enables interactions within a volume of 0.2 m^3, approximately shaped as an inverted pyramid from its internal cameras. In static situations, it can record fingertip positions with a sub 0.5 mm standard deviation.[52] However, for dynamic scenarios, inconsistent and unreliable values have been obtained, especially for tracking objects further than 300 mm from the sensor and at the extremities of its field of view.[52,53] So, in this work, the sensor was used for interactions within a workspace volume of $\approx 200 \times 200 \times 200$ mm^3.

As that sensor is designed to detect naked fingers, the presence of a tactile display on each fingertip was an issue that needed to be addressed. Specifically, according to the sensor's principle of operation (stereo image comparison of an infrared illuminated scene), the casing required an optical reflecting signature not too dissimilar from that of a fingertip's skin. To address that need, various test casings were manufactured with different 3D printed polymers. The best tracking results could be achieved with materials having a semi translucent or light color, without a gloss finish. The final casing was produced with a translucent resin (see the Experimental Section).

The encased display had a maximum thickness of 12 mm and a width of 20 mm, which matched the average width of thumb and index fingers across the pool of volunteers used for the psychophysical study described later on in the paper. In order to easily secure the casing to the fingertip, without precluding optical tracking by the sensor, the structure was fitted with transparent elastic straps (see the Experimental Section). The weight of a fingertip-mounted display was 6 g.

The device was driven with voltages up to 4 kV. In an early design of this display, such voltages were applied via a low-to-high-voltage DC–DC converter arranged (together with a high-voltage discharge resistor) on the frontal part of the plastic casing.[47] Although that solution avoided the need for an external high-voltage unit and high-voltage connecting cables, it made the wearable display rather cumbersome and unsuitable for multifinger systems. To overcome that drawback, in this work we opted for a desktop high-voltage control box, whose custom implementation is shown in Figure 1f (see details in the Experimental Section).

The following sections present a characterization of the electromechanical performance of the display, in terms of achievable forces and displacements, as well as a psychophysical investigation on its tactile feedback performance.

4.2. Blocking Force Performance

In order to determine the force output as a function of the applied voltage, a blocking force test was performed with a circular flat-faced indenter having a diameter of 12 mm, which was slightly smaller than the HC-DEA base diameter (12.5 mm). The test was made as represented in **Figure 2**a and detailed in the Experimental Section, on different tactile displays made of membranes with one, two, three, or four layers of dielectric elastomer film. Results are presented in Figure 2b.

As expected, the multilayer structure increased the force output, without changing the driving voltage range. For membranes made of four layers, the maximum force was 1 N. As a comparison, a previous version of the device, with a single-layered membrane and a base diameter of 20 mm, produced (on the same circular indenter of 12 mm) a maximum blocking force of 0.6 N.[47]

4.3. Static and Dynamic Free-Stroke Performance

The various tactile displays with membranes made of a different number of layers were also studied with a free-stroke test. To that end, the passive membrane's vertical displacement was measured using the set-up represented in Figure 2a and detailed in the Experimental Section. Results are presented in Figure 2c. As expected, the increased number of layers had a practically negligible impact on the free stroke. Indeed, despite an increase of the membrane's thickness and an associated higher stiffness, each internal electroded layer experienced an electric field and, so, an electrostatic stress (Equation 1), that was practically identical to that related to a mono-layer structure.

Nevertheless, it is also worth noting that a slight reduction in displacement for the increasing number of layers can be distinguished at the highest end of the voltage range (Figure 2c), where the deformations are largest. This is evidence that the different constraints of each layer when it is part of a stack, as compared to when it is alone, have an effect on the resulting deformation.

The dynamic performance was assessed by characterizing the frequency response, in terms of free stroke induced by unipolar square-wave voltage signals having constant amplitude of 3.5 kV and a variable frequency in the range 0.1–3 Hz. For each frequency, the difference between maximum and minimum displacements was averaged over the first five cycles. Results are reported in in Figure 2d. Whilst in the lowest part of the frequency range the responses overlapped, a drop off for increasing layers progressively showed up toward the highest end of the range. This might be due to several interplaying factors, including an increase of both the mechanical and electrical time constants for an increasing number of layers.

As a consequence of the lowering of the curves for increasing layers, the cut-off frequency corresponding to a −3 dB drop of the response from its low-frequency value was found to reduce,

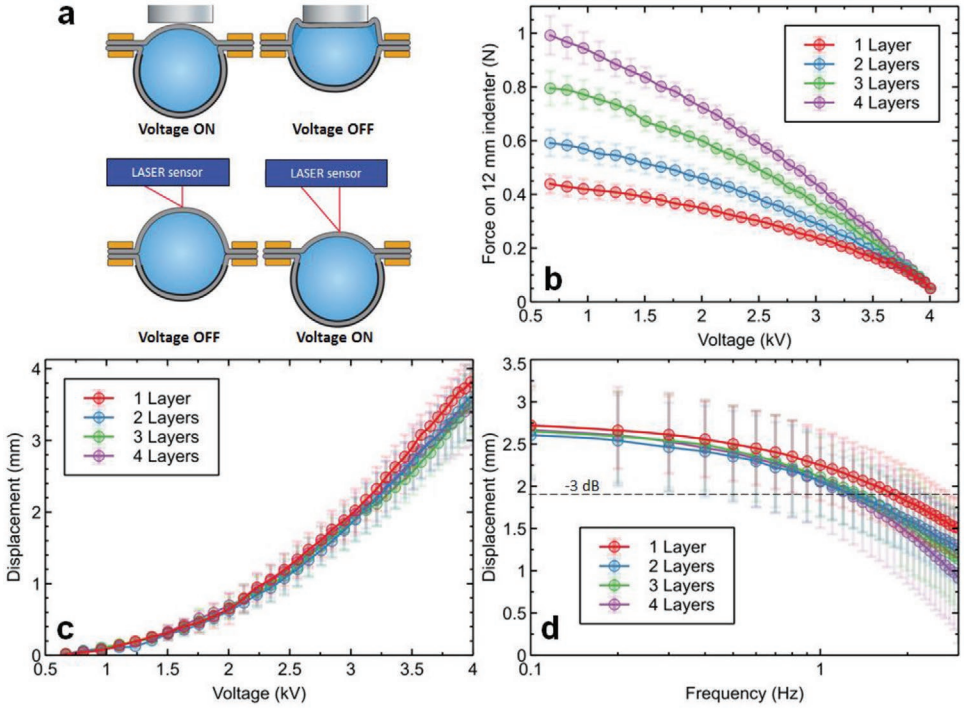

Figure 2. Electromechanical performance of different tactile displays made of membranes with a different number of layers. a) Schematic drawings of the experimental set-up used to measure the tactile display's blocking force (top) and free stroke (bottom); b) Blocking force as a function of the applied voltage; c) Free stroke as a function of the applied voltage; d) Frequency response, in terms of difference between maximum and minimum free-stroke displacements in response to a unipolar square wave at 3.5 kV. In each plot, the error bars represent the standard deviation among three samples of each display type.

although it remained confined between 1 and 2 Hz (Figure 2d). Such a limited bandwidth was mostly due to two main factors: i) a low response speed of the membrane's elastomeric material (VHB acrylic, by 3M), caused by its well-known viscoelastic losses arising from a high viscosity, relative to other materials, such as silicones;[54] and ii) the low bandwidth of the DC–DC high-voltage converter used to drive the actuator (see the Experimental Section).

4.4. Psychophysical Assessment of the Tactile Feedback Performance

A psychophysical study was conducted on fifteen volunteers (eight males and seven females, aged between 21 and 29). The tactile display (made of three-layered membranes) was used in combination with the LEAP Motion hand tracking system described above, in front of a computer screen, in order to enable visuo–tactile interactions with an ad-hoc created virtual environment. Custom control software was developed for the tests, as detailed in the Experimental Section.

Each volunteer was engaged in three independent experiments. Each of them envisaged a specific kind of interaction with two virtual objects ('A' and 'B'), which alternatively appeared on the left or right sides of the screen, depending on where the user was pointing the hand. The movements of the fingertips were tracked in real time and mapped on the virtual environment via a rudimental 'avatar,' simply consisting of two spheres (purple color in **Figure 3**), smaller than the object (green color in Figure 3) and able to interact with it. So, by moving the hand and one or two fingertips equipped with the display, the user could navigate the virtual environment, seeking for a contact with the object. The tactile interaction triggered a response of the display, as a tactual stimulus generated on the finger pulp by an actuation voltage within the 0–4 kV range. The user was asked to probe the two objects more than once and to compare the tactile feedback. No restriction was applied to the exploration time, allowing users to compare the two stimuli as long as needed.

The experiments differed according to the number of fingers involved (one or two), the way of probing the object (poke or pinch), and the type of perceived stimulus (force or compliance), as described below.

4.4.1. First Experiment: Single Finger Poke

The user wore a tactile display on the index finger and was asked to poke two circles, alternatively appearing on the left and right sides of the screen. As soon as the fingertip's avatar entered the circle, the latter changed color and the tactile display was actuated with a constant voltage, which was maintained as long as the finger remained inside the circle. As a result, the tactile stimulus on each circle consisted of a constant force (corresponding also to a constant indentation of the finger pulp and a constant contact area with it). In a sequence of trials, the two circles were randomly associated to different voltages and each time the user was asked to indicate which circle

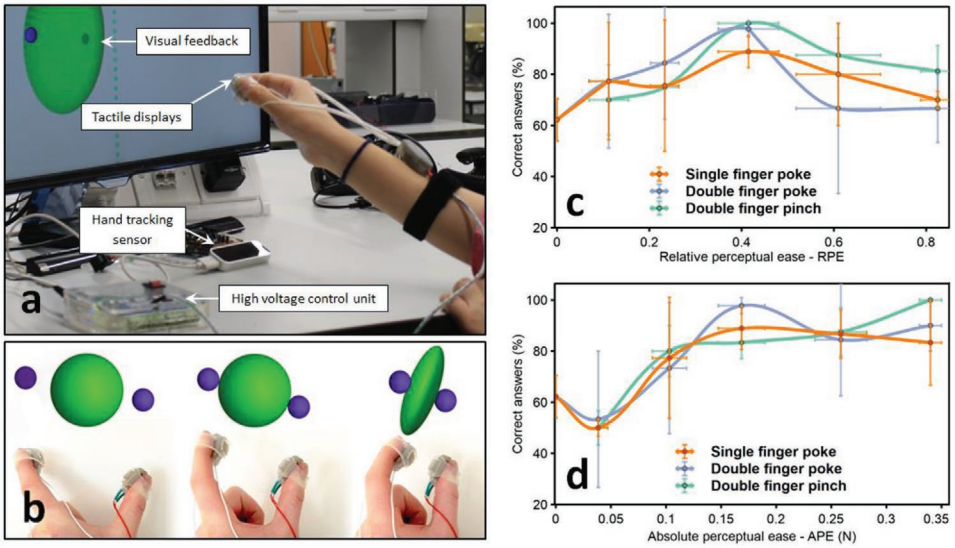

Figure 3. Psychophysical assessment of the tactile feedback performance. a) Experimental set-up, consisting of the tactile displays on the fingertips, the high-voltage control unit, the LEAP Motion hand tracking sensor, the visualization screen, and a processing computer; b) Pinch gesture to explore the softness of a virtual ball; a video of a demo can be watched at https://www.youtube.com/watch?v=vj_wsnQt8So; c,d) Rate of recognition in comparing two tactile stimuli, as a function of the relative (c) or absolute (d) ease of the perceptual discrimination task, for each experiment. The vertical error bars represent the standard deviation among answers collected from three comparative tasks performed by each of the 15 volunteers. The horizontal error bars represent the standard deviation among the perceptual ease values included in each group represented by the average value. Note that, as the RPE grouping was different than the ABE grouping, the average correct answers for each group changed, such that the variation range of correct answers for each experiment slightly differed between the two graphs.

provided the highest/lowest force, or if no noticeable difference could be appreciated.

4.4.2. Second Experiment: Double Finger Poke

The user was presented with the same kind of visuo–tactile feedback and had to perform the same comparative task as in the first experiment, although in this case two tactile displays were used: one on the thumb and the other one on the index finger, of the dominant hand. The user had to enter each circle with both fingers (Figure 3a) and the two displays simultaneously rendered the same force. As for the first experiment, the two circles were randomly associated to different voltages and the user had to indicate which circle provided the highest/lowest force, or if no noticeable difference was appreciated.

4.4.3. Third Experiment: Double Finger Pinch

While wearing two tactile displays (on the thumb and index finger), the user was asked to pinch two deformable balls, alternatively appearing on the left and right sides of the screen. Pinching to a larger extent corresponded to a visualization of the ball with a greater squeeze, accompanied by a generation of a higher tactile force. In order to facilitate the task, the ball was always visualized between the two fingers (Figure 3b), so as to maximally focus attention on the tactile sensation.

For each participant, the system was initially calibrated, using the fully open pinch position. Force was only rendered when the distance between the thumb and index finger (pinch distance) was between ¾ and ¼ of that recorded in the fully open position. Within that range, the voltage was decreased (linearly, for simplicity), so as to vary the force from null to maximum and, so, to mimic a certain compliance. Moreover, in order to (randomly) vary the rendered compliance, the voltage was varied with a different derivative with respect to the pinch distance. The user was asked to indicate which ball was perceived as the softest/hardest, or if no noticeable difference could be appreciated.

4.4.4. Perceptual Discrimination Assessment

In order to evaluate the perceptual performance, it was necessary to define, first, a metric to quantify the ease of any perceptual discrimination task. This aimed to define how easily the two tactile stimuli from the virtual objects 'A' and 'B' were expected to be distinguishable, according to the human tactile perception, regardless of the tactile display performance. Then, the latter was evaluated, relative to the ease of the comparative task.

In order to define such a metric, we first considered the Weber's law: in general, the just noticeable difference between a certain stimulus and a variation of it is a constant proportion of the original stimulus magnitude.[55] Therefore, the higher a stimulus, the greater the changes required so that they can be distinguished. According to this, a possible metric, here called 'ideal relative perceptual ease' (RPE_{ideal}) of the comparative task, could be defined as follows:

$$RPE_{ideal} = |S_A - S_B| / S_{max} \quad (2)$$

where $|S_A - S_B|$ is the absolute difference between the two stimuli S_A and S_B presented in the comparative task and S_{max} is the maximum value between them. In the experiments, each stimulus was either a force (poke experiments) or a compliance (pinch experiment). Due to the fact that, according to the Weber's law, for decreasing values of S_{max} the just noticeable difference decreased, it was expected that also any given difference $|S_A - S_B|$ was easier to recognize for decreasing values of S_{max}. So, in other words, the higher PE_{ideal}, the easier the comparative task was expected to be.

Nevertheless, in the experiments the tactile displays were neither force nor compliance controlled, as they were driven by a controlled voltage. So, the RPE_{ideal} could not be calculated and an approximated estimate was obtained as follows. For each stimulus, the driving voltage (for the pinch experiment it was the value corresponding to the lowest pinch distance) was used to calculate, from the data in Figure 2b, the equivalent force on the 12-mm indenter used in the characterisation tests. The so-obtained equivalent force couples F_A and F_B for each comparative test were used to estimate the RPE of the comparative task, as follows:

$$RPE = |F_A - F_B| / F_{max} \quad (3)$$

where F_{max} was the maximum force between F_A and F_B. Therefore, growing values of RPE consistently corresponded to growing values of RPE_{ideal}.

In order to analyze the comparison outcomes in each experiment, the tests were clustered such that those having close RPE values were grouped together and their average RPE was considered. Then, for each average RPE, the average percentage of correct answers was calculated.

Results are presented in Figure 3c. For each experiment, the number of correct answers substantially showed a maximum at a given RPE, which was not the highest tested value. The fact that each curve did not show a substantially growing trend, up to the highest RPE, was unexpected, according to the significance of RPE.

In order to clarify whether that outcome was due to a (unexplainable) poor performance of the tactile display technology at high RPE values (i.e., exactly in the range where the comparative tasks were expected to be easier), or to a methodological flaw, the data were evaluated also according to a different metric of the perceptual ease of the comparative task. This was called 'absolute perceptual ease' (APE) and defined as follows:

$$APE = |F_A - F_B| \quad (4)$$

By grouping close APE values and plotting the average percentage of correct answers for each group, the new graph shown in Figure 3d was obtained. As expected, for each experiment the recognition rate was found to substantially increase with the APE of the task. Indeed, a growing difference between the stimuli facilitated their discrimination.

Therefore, the drop observed in the recognition rate at high RPE values (Figure 3c) was not due to poor performance of the technology, but, rather, to a misuse of RPE as a metric presumably applicable to any level of stimulus. Indeed, high RPE values were obtained not only from large variations of intense stimuli (which were actually easy to recognise), but also from small variations of tiny stimuli, close to the perceptual threshold, which therefore were difficult to distinguish. The latter cases determined higher errors of discrimination, such that the total percentage of correct answers dropped down. This indicates that the RPE could not be considered as fully representative of the actual ease of a comparative task.

The use of APE as a more appropriate metric showed a correlation between the ease of the tasks and the actual ability of users to correctly compare the presented tactile stimuli. In particular, at APE > 0.1 N, the recognition rate was higher than 80% for all the experiments, and at an APE ≈ 0.34 N it reached 100% for the pinch experiment (Figure 3d). These results are indicative of an ability of the tactile display to generate adequate tactile feedback, which allowed volunteers to recognise different stimuli, with an accuracy correlated to a variable complexity of the comparative task.

5. Future Developments

5.1. Further Increases of the Force

The multilayer approach adopted in this work was shown to be effective to increase the achievable force. Whilst additional layers could be added to increase this further, preliminary tests showed that the growing pressurization of the fluid necessary with an increasing number of layers could create leakage from the interface between the passive and active membranes. So, using a higher number of layers would require improving adhesion between the membranes. This could be achieved via physical or chemical approaches. For instance, for the case of membranes made of silicone (as discussed below), it is known that bonding can be enhanced by surface activation with oxygen plasma, which has been shown to be effective in different types of DEAs.[54]

5.2. High Voltages: Implications on Safety, Size, and Cost

The main limitation of this tactile display technology is the need for high driving voltages, which has the implications discussed below.

In terms of electrical safety, dealing with voltages in the kV range is clearly not desirable. However, this drawback is mitigated not only by the actuator's unique design (separation between the fingertip and the high-voltage membrane via a large insulating chamber and a passive membrane), but, especially, by the fact that there is no need for a high driving power (as the electrical load is capacitive). This feature allows for using electrically safe driving sources, such as the DC–DC voltage converter employed in this work, which provided a maximum power of 0.5 W.

The low power requirement favors the adoption of relatively compact high-voltage components. For instance, the DC–DC converter was a 13 mm-sided cube. Such a size enables the development of portable electronics. However, that size can still be excessive for specific applications, such as those that target multifinger operation and fully wearable systems.[47] In order

to address this need for further miniaturization, one strategy could be, for instance, to implement a multiplexing of driving signals, through high-voltage transistors, from a single high-voltage source.

Nevertheless, regardless of the driving strategy, any electronics working in the kV range will always be bulkier (due to need for insulations) and more expensive (especially due to a lower market share) than any electronics working at one-order-of-magnitude lower voltages. So, for a major breakthrough, a reduction of the driving voltage to a few hundred volts is imperative. This need can be addressed as discussed below.

5.3. Strategies to Reduce the Driving Voltages

Lowering the driving voltage should target a reduction below the threshold of 500 V, as in that range highly compact electronics suitable to drive DEAs has been demonstrated.[36] Furthermore, a few hundred volts are typical for the low-cost and low-size electronics of common piezoelectric actuators. In order to reach that goal, according to Equation 1 there are two strategies: i) a long-term approach is at a material development level and concerns the synthesis of new elastomers with a higher dielectric constant;[56,57] and ii) a short-term approach is at a material processing level and concerns the fabrication of dielectric elastomer membranes with a lower thickness.

In order to meet those needs, the best materials of choice (in several respects, including reliability, versatility, and low cost) today are silicone elastomers. Even with off-the-shelf compositions, it has already been shown that it is possible to reduce the thickness of soft insulating membranes to a few microns, while preserving actuation capability.[36,58] This evidence suggests that the DEA technology in general might soon rather use more compact and cost-effective electronics.

Nevertheless, such a technological trend toward films with lower thickness implies the need for stacking more layers to preserve the elastic force of the resulting membranes. So, multilayer manufacturing processes will likely have a growing importance in the future of this actuation technology.

5.4. Strategy to Extend the Frequency Response

The envisaged use of silicones in the future will also address a limitation that affects the 3M VHB poly-acrylic elastomer adopted in this work. Although it is one of the most studied soft insulators for DEAs,[31–33] as it facilitates prototype fabrication and is capable of large electromechanical strains and stresses, it has a well-known poor viscoelastic performance, which causes significant creep and stress relaxation.[59] The elastomer was also used in the early versions of this tactile display, whose stress relaxation was characterized.[47]

As silicones typically have at room temperature a lower loss modulus, they lead in general to DEAs with more stable and also faster response.[54] So, silicones represent at present the best strategy to extend the bandwidth also of the tactile display presented here. Nevertheless, so far, DEAs made of off-the-shelf silicones have demonstrated, when compared to VHB-based devices, lower electromechanical strains and stresses, mainly due to a significantly lower dielectric strength, which limits the maximum electric fields applicable. This means that, until reliable improved formulations are available, the use of conventional silicones will imply the need for accepting a trade-off between electromechanical and viscoelastic performance.

5.5. Strategy to Control the Displayed Softness

Like any other wearable tactile display of softness described so far, this device can vary the contact area with the fingertip (and so also the displayed softness) only in open-loop mode. In order to achieve closed-loop controllability, via a real-time monitoring of the contact area, two approaches can be considered: model-based control and sensing-based control, as discussed below.

The former would require an accurate physical model, capturing the complexity of the contact mechanics arising from the deformability of both the display and fingertip. Owing to the visco-hyper-elastic nature of both of them, the problem should be addressed with numerical investigations, extending, for instance, approaches analogous to that described in.[60] The model should consider the variability of the mechanical parameters within the involved ranges of deformation and frequency. Although it has been suggested that perceptual compensations for the finger deformability might occur while judging softness, such that the finger could be considered as rigid,[11] it is possible that such an assumption might not be accurate at any indentation range. Indeed, the finger pulp's stiffness changes with the intensity of the compression. An accurate model then would imply the need for identifying visco-hyper-elastic and geometrical parameters, which cannot be user-specific (for practical reasons) and have to be extracted by fitting data from a statistically significant population. The accuracy of such parameters for controlling the contact area on different individuals should then be validated. This would then raise the challenge on how to measure the contact area for the validation experiments. One option could consist in covering the membrane with a dye and measuring the stain on the finger, although more accurate methods would be preferable.

A way to avoid such a complexity of a model-based approach is to integrate into the device passive membrane an array of distributed sensors for contact area detection. However, no sensing technology today appears to be sufficiently mature to combine a high spatial resolution with an ease of reading on a soft membrane undergoing large deformations. Indeed, although distributed-sensing could be achieved by covering the membrane with an array of stretchable resistors or capacitors, the detection accuracy would depend on the surface density of the tactile elements ("tactels"). The higher the density, the greater the complications that occur, especially for routing the necessary stretchable electrical connections to read each tactel.

Such a problem is in general addressed by ongoing research on new strategies to read arrays of deformable sensors. As an example, it has recently been shown that a set of elastomeric capacitors and connections can be replaced by a stack of two elastomeric capacitive membranes and a multifrequency capacitance reading.[61] Although such an approach is attractive to avoid the need for physically addressing each tactel, achieving this at high resolutions appears challenging, owing to the small

differences of capacitances to be resolved between adjacent elements.[61]

Such evidence suggests that future developments of these tactile displays, as well as those using different ways to deform a soft membrane (such as pneumatically[25]), should address the need for investigating the best strategy to achieve contact area sensing. The required resolution is still unknown. Although in finger pads the tactile resolution can be as low as ≈0.3 mm (owing to tactile hyperacuity[62,63]), studies are needed to evaluate whether a virtual softness can effectively be rendered by controlling the contact area, with a lower accuracy.

6. Conclusions

This work described compact tactile displays made of electroresponsive elastomers, capable of mimicking non-vibratory tactual interactions with soft bodies. Forces up to 1 N and displacements up to 3.5 mm could be generated with a 6 g device, made of four-layered membranes. The size and shape of the display made it easy to wear on individual fingertips, without precluding an optical tracking of finger motions. When combined with a low-cost and compact hand tracking sensor, this made it possible to demonstrate a simple and cost-effective virtual-reality system.

A psychophysical investigation showed that users could properly distinguish between different stimuli rendered by the device, with a degree of accuracy correlated to the perceptual difficulty of the tactile discrimination task.

Possible improvements of this technology have been discussed, highlighting pros and cons of different approaches.

7. Experimental Section

Dielectric Elastomer Membranes: The dielectric material used for the active and passive membranes consisted of an acrylic elastomeric film (VHB 4910, 3M, USA). Prior to providing them with a dome-like shaping (see below), the films were biaxially prestrained by 350% (i.e., biaxially prestretched by 4.5 times). As a result, their thickness decreased from initial 1000 μm to a (calculated) value of ≈50 μm. It is worth noting that, although higher prestrains were demonstrated to be optimal for VHB-based DEAs working in planar mode,[64] in this work the prestrain was limited, in consideration of the non-planar configuration assumed by the membranes. Indeed, for higher prestrains, the active membranes could become more prone to electrical breakdown and mechanical fracture failure, as a result of an excessive thinning, due to three factors: 1) their dome-like shaping during manufacture; 2) their further passive stretching, caused by the user while wearing the device; and 3) their further active stretching, caused by the applied electric field while activating the device. Empirically, it was found that 350% was an adequately safe prestrain, although it was not optimized, thereby leaving room for possible improvements in the future.

Compliant Electrodes: Stretchable electrodes were created on either side of each layer of the active membrane, using a silicone/carbon black composite. A carbon black powder (Black pearl 2000, Cabot, USA) was added at a 9 wt% ratio to an uncured silicone prepolymer mixed with its curing agent (CF19-2186, Nusil, USA). Following a masking of the prestretched elastomer membranes with a paper stencil, the silicone/carbon black mixture was applied to the VHB film using an airbrush. The mixture was cured at room temperature for 10 min. The resulting compliant electrodes had an average sheet resistance of 45 kΩ sq^{-1}, as measured according to the procedure described by the standards for DE transducers.[65]

Rigid Support Frames: The passive and active membranes were coupled to two rigid support frames (Figure 1d), fabricated from 0.5 mm-thick laser-cut acrylic sheets. The frame had a hole with a diameter identical to the intended base diameter of the final device. The plastics surrounding the hole had a width of 2.5 mm, so as to leave a sufficient annular planar area for adequate bonding between the passive and active membranes during the manufacturing process of the device (lower sizes were found to lead to fluid leakage). The frames were designed to integrate fixing bolts (Figure 1e), which penetrated the electrodes, offering a robust and safe method to secure the electrodes to the high-voltage wires, as well as the whole actuator to its casing.

Tactile Display Assembly: The bubble-like HC-DEA with the intended number of layers for both the active and passive membranes was manufactured using the same procedure described in ref. [46]. The passive membrane was created by prestretching the constitutive VHB film (see above) on a large frame. In order to obtain a multilayer membrane, the process was repeated by manually stacking multiple prestretched films. The resulting membrane was then transferred to the smaller rigid support frame described above and placed over a small vacuum chamber having a circular hole, identical to that of the rigid support frame. A depressurization was applied in order to deform the membrane and create a cavity, which was then filled in with an insulating silicone grease (8462, M.G. Chemicals, Canada) acting as the coupling fluid. The grease-filled cavity was then closed with the active membrane, planarly arranged on top of it. The active membrane was obtained by manually stacking the same number of layers of prestretched VHB films (see above) used for the passive membrane, although an electrode layer was created (see above) on either side of each VHB layer. A second rigid plastic frame, identical to the first one, was finally applied above the active membrane. The adhesiveness of the VHB film allowed for proper bonding. After 10 min, the chamber was repressurized and the coupled membranes (with the fluid confined between them) were detached from the chamber, obtaining, after a relaxation of the membranes, a symmetrical bubble-like HC-DEA. The actuator was then fitted into a plastic casing (Figure 1e), which was 3D printed (Object 30-Pro, Stratasys, USA) using a translucent resin (VeroClear-RGD810, Stratasys, USA). The casing was secured to the fingertip via transparent elastic straps, which were produced by mould-casting with a thickness of 1.5 mm, using a transparent silicone (Transil 40–1, Mouldlife, UK).

High-Voltage Control Electronics: A four-channel desktop control unit was assembled, using one DC–DC converter (EMCO Q50, EMCO High Voltage, USA) for each channel. Each converter was fed with a 0.7–4.0 V signal, to generate a voltage up to 4 kV. It is worth noting that the minimum input voltage was 0.7 V, as this was found to be the lower limit of the converter's linearity range. In order to enable a control of multiple displays independently, a microcontroller (Arduino Micro, Arduino, Italy), based on the microprocessor ATmega32U4, was used. The microcontroller was capable of controlling up to seven 8-bit pulse width modulated (PWM) channels, with a PWM cycle frequency of 490 Hz. In order to smooth the PWM signal, a low pass filter (made of a 4.7 μF capacitor and a 150 Ω resistor) was used, enabling an almost linear control of the high-voltage driving signal. Due to its high input current demand, each DC–DC converter was driven with a voltage follower (buffer), which was implemented with an integrated amplifier (TCA0372, ON Semiconductor, USA), powered by an external regulated 5V–1A power supply. A Schottky diode was placed in series to each converter's input, so as to avoid back voltages. Moreover, a high-voltage discharge resistor of 200 MΩ was arranged in parallel to each converter's output, in order to both let the converter to work with proper electrical loading and allow the actuator to be quickly discharged.

Blocking Force Test: The test was performed with a universal mechanical testing machine (3300 single column, Instron, USA), equipped with a 10 N load cell (2519-10N, Instron, USA) connected to a circular 12 mm-diameter flat-faced indenter. The set-up is represented in Figure 2a. At the start of each test, the actuator was deformed through the application of 4 kV. The applied voltage caused the actuator's passive membrane to move downward, until it was almost flat and aligned with the top rigid support frame. The indenter was then lowered

onto the deformed passive membrane until contact was established. Contact was defined as the condition corresponding to an offset force of ≈0.05 N (empirically chosen, relative to the load cell's sensitivity). Once this offset value was reached, the actuation voltage was dropped from 4 to 0.7 kV, over a 10 s period, with steps of ≈103 V every 0.29 s. Force data were collected at a rate of 100 Hz, corresponding to 29 samples per voltage step, which were then averaged to produce a single force value for each step. The rate at which the voltage was decreased across the actuator was selected in order to gain suitable sampling accuracy from the load cell. The test was repeated five times for each display tested.

Free-Stroke Test: The passive membrane's vertical displacement was measured with a LASER sensor (optoNCDT ILD 1402–5, Micro-epsilon, Germany). The set-up is represented in Figure 2a. Measurements were taken as the actuation voltage was increased from 0.7 to 4 kV over a 10 s period, with steps of ≈103 V every 0.29 s. Displacement data were collected at a rate of 100 Hz, corresponding to 29 samples per voltage step, which were then averaged to produce a single displacement value for each step.

Control Software for the Psychophysical Tests: A custom control program running on an external desktop computer was developed to perform the following tasks: continuously track the position of the fingertips wearing the tactile displays, detect collisions of the virtual fingertips with the virtual objects, and generate the described tactile and visual feedback on the fingers and computer screen. Interfacing with the LEAP Motion tracking sensor was achieved using the software library LEAP Motion SDK version 2.3.1. Java version 8.0 was used as the programming language, with the graphical user interface windows being facilitated by the Processing 3.0 Java library. The control signals for the tactile displays were sent from the computer, through a wired USB connection, to an Arduino Micro, which controlled the actuators, as described above. This was achieved through the Arduino Firmata firmware library running on the microcontroller, and the Java RXTX serial communication library, which was used as the interface protocol between the computer and the microcontroller. The program refreshed at a frame rate of ≈60 Hz, running on a Linux-based operating system with an 8 GB random access memory and a 3.2 GHz processor.

Psychophysical Tests Approval: The psychophysical tests were approved by the Queen Mary Ethics of Research Committee prior to the research (QMREC1567 – 'Psychophysical characterization of a wearable tactile display') and informed written consent was obtained from all participants.

Acknowledgements

This work was partially supported by the UK EPSRC (Engineering and Physical Sciences Research Council) and the UK AHRC (Arts and Humanities Research Council) Centre for Doctoral Training in Media and Arts Technology (EP/L01632X/1), by the European Commission's MSCA-ITN-2014 Marie Sklodowska-Curie Innovative Training Network Programme ("MICACT – MICroACTuators" project, grant agreement 641822), and by the Italian Tuscany Region's POR FESR 2014–2020 Programme ("BMI Focus", RS2017, Regione Toscana, D.D. n.7165 del 24/5/2017).

Conflict of Interest

The authors declare no conflict of interest.

Data Availability Statement

The data that support the findings of this study are available from the corresponding author upon reasonable request.

Keywords

actuators, dielectric elastomers, soft, tactile displays, wearables

Received: January 8, 2021
Published online:

[1] N. E. Seymour, A. G. Gallagher, S. A. Roman, M. K. O'Brien, V. K. Bansal, D. K. Andersen, R. M. Satava, *Ann. Surg.* **2002**, *236*, 458.
[2] I. Sarakoglou, N. Garcia-Hernandez, N. G. Tsagarakis, D. G. Caldwell, *IEEE Trans. Haptics* **2012**, *5*, 252.
[3] X. Liu, G. Dodds, J. Mc Cartney, B. Hinds, *Comput.-Aided Des.* **2004**, *36*, 1129.
[4] A. Seth, J. Vance, J. Oliver, *Virtual Reality* **2011**, *15*, 5.
[5] S. Oh, J. N. Bailenson, G. F. Welch, *Front. Rob. AI* **2018**, *5*, 114.
[6] M. A. Srinivasan, R. H. LaMotte, *J. Neurophysiol.* **1995**, *73*, 88.
[7] A. Bicchi, E. P. Scilingo, D. De Rossi, *IEEE Trans. Rob. Autom.* **2000**, *16*, 496.
[8] K. Fujita, H. Ohmori, in *Proc. of 5th World Multiconference on Systemics, Cybernetics, and Informatics* (Ed: N. Callos), Cybernetics and Informatics, Orlando, Florida **2001**.
[9] W. M. B. Tiest, A. M. L. Kappers, *IEEE Trans. Haptics* **2009**, *2*, 189.
[10] A. Moscatelli, M. Bianchi, A. Serio, V. Hayward, M. O. Ernst, A. Bicchi, *Curr. Biol.* **2016**, *26*, 1159.
[11] C. Dhong, R. Miller, N. B. Root, S. Gupta, L. V. Kayser, C. W. Carpenter, K. J. Loh, V. S. Ramachandran, D. J. Lipomi, *Sci. Adv.* **2019**, *5*, eaaw8845.
[12] C. Pacchierotti, A. Tirmizi, D. Prattichizzo, *ACM Trans. Appl. Percept.* **2014**, *11*, 4.
[13] M. Gabardi, M. Solazzi, D. Leonardis, A. Frisoli, in *2016 IEEE Haptics Symp.*, IEEE, Philadelphia **2016**, pp. 140–146.
[14] E. M. Young, K. J. Kuchenbecker, *IEEE Trans. Haptics* **2019**, *12*, 295.
[15] A. G. Perez, D. Lobo, F. Chinello, M. Malvezzi, G. Cirio, J. S. Martın, D. Prattichizzo, M. A. Otaduy, *IEEE Trans. Haptics* **2017**, *10*, 254.
[16] A. Girard, M. Marchal, F. Gosselin, A. Chabrier, F. Louveau, A. Lécuyer, *Front. ICT* **2016**, *3*, 6.
[17] H. Kim, H. B. Yi, H. Lee, W. Lee, in *Proc. of 2018 CHI Conf. on Human Factors in Computing Systems*, Association for Computing Machinery, New York **2018**, pp. 1–13.
[18] C. Pacchierotti, S. Sinclair, M. Solazzi, A. Frisoli, D. Prattichizzo, V. Hayward, *IEEE Trans. Haptics* **2017**, *10*, 580.
[19] Y. Tanaka, H. Yamauchi, K. Amemiya, *Proc. JFPS Int. Symp. Fluid Power* **2002**, *2002*, 309.
[20] Y. Kim, I. Oakley, J. Ryu, in *2006 SICE-ICASE Int. Joint Conf.*, IEEE, Philadelphia **2006**, pp. 1933–1938.
[21] T. Taniguchi, S. Sakurai, T. Nojima, K. Hirota, in *Haptics: Science, Technology, and Applications* (Eds: D. Prattichizzo, H. Shinoda, H. Tan, E. Ruffaldi, A. Frisoli), Springer, Cham, Switzerland **2018**, pp. 58–67.
[22] C.-H. King, M. Franco, M. O. Culjat, A. T. Higa, J. W. Bisley, E. Dutson, W. S. Grundfest, *J. Med. Devices* **2008**, *2*, 041006.
[23] Y. L. Feng, R. L. Peiris, C. L. Fernando, K. Minamizawa, in *Haptics: Science, Technology, and Applications* (Eds: D. Prattichizzo, H. Shinoda, H. Tan, E. Ruffaldi, A. Frisoli, Springer, Cham, Switzerland **2018**, pp. 180–192.
[24] G. Moy, C. Wagner, R. S. Fearing, in *Proceedings 2000 ICRA. Millennium Conf. IEEE Int. Conf. on Robotics and Automation. Symposia Proceedings*, IEEE, Philadelphia **2000**, pp. 3409–3415.
[25] G. Frediani, F. Carpi, *Sci. Rep.* **2020**, *10*, 20491.
[26] T. Endo, A. Kusakabe, Y. Kazama, H. Kawasaki, *IEEE/ASME Trans. Mechatronics* **2016**, *21*, 2343.
[27] S. Fani, S. Ciotti, E. Battaglia, A. Moscatelli, M. Bianchi, *IEEE Trans. Haptics* **2018**, *11*, 304.
[28] K. Song, S. H. Kim, S. Jin, S. Kim, S. Lee, J.-S. Kim, J.-M. Park, Y. Cha, *Sci. Rep.* **2019**, *9*, 8988.

[29] E. Leroy, R. Hinchet, H. Shea, *Adv. Mater.* **2020**, *32*, 2002564.
[30] I.-D. Sîrbu, G. Moretti, S. Dirè, L. Fambri, R. Vertechy, D. Meniglio, M. Fontana, in *Proceedings of SPIE* (Ed: Y. Bar-Cohen), SPIE, Bellingham, WA **2019**, pp. 334–339.
[31] P. Brochu, Q. Pei, *Macromol. Rapid Commun.* **2010**, *31*, 10.
[32] *Dielectric Elastomers as Electromechanical Transducers* (Eds: F. Carpi, D. De Rossi, R. Kornbluh, R. Pelrine, P. Sommer-Larsen), Elsevier, Oxford **2008**.
[33] R. Pelrine, R. Kornbluh, Q. Pei, J. Joseph, *Science* **2000**, *287*, 836.
[34] *Electromechanically Active Polymers* (Ed: F. Carpi), Springer, Zurich **2016**.
[35] F. Carpi, S. Bauer, D. De Rossi, *Science* **2010**, *330*, 1759.
[36] X. Ji, X. Liu, V. Cacucciolo, Y. Civet, A. E. Haitami, S. Cantin, Y. Perriard, H. Shea, *Adv. Funct. Mater.* **2020**, 2006639.
[37] M. Matysek, P. Lotz, T. Winterstein, H. F. Schlaak, in *World Haptics 2009 - Third Joint EuroHaptics Conf. and Symp. on Haptic Interfaces for Virtual Environment and Teleoperator Systems*, IEEE, Philadelphia **2009**, pp. 290–295.
[38] H. Phung, C. T. Nguyen, T. D. Nguyen, C. Lee, U. Kim, D. Lee, H. Moon, J. C. Koo, H. R. Choi, *Meccanica* **2015**, *50*, 2825.
[39] H. Phung, C. T. Nguyen, H. Jung, T. D Nguyen, H. R. Choi, *Smart Mater. Struct.* **2020**, *29*, 035007.
[40] E. Knoop, J. Rossiter, *Smart Mater. Struct.* **2015**, *24*, 045034.
[41] K. W. Jun, J. N. Kim, I.-K. Oh, *Small* **2018**, *14*, 1801603.
[42] A. Ankit, N. Tiwari, M. Rajput, N. A. Chien, N. Mathews, *Small* **2018**, *14*, 1702312.
[43] H. Prahlad, R. Pelrine, R. Kornbluh, P. von Guggenberg, S. Chhokar, J. Eckerle, M. Rosenthal, N. Bonwit, in *Proceedings of SPIE* (Ed: Y. Bar-Cohen), SPIE, Bellingham, WA **2005**, pp. 102–113.
[44] I. M. Koo, K. Jung, J. C. Koo, J. D. Nam, Y. K. Lee, H. R. Choi, *IEEE Trans. Rob.* **2008**, *24*, 549.
[45] S. Mun, S. Yun, S. Nam, S. K. Park, S. Park, B. J. Park, K. U. Kyung, *IEEE Trans. Haptics* **2018**, *11*, 15.
[46] F. Carpi, G. Frediani, D. D. Rossi, *IEEE/ASME Trans. Mechatronics* **2010**, *15*, 308.
[47] G. Frediani, D. Mazzei, D. D. Rossi, F. Carpi, *Front. Bioeng. Biotechnol.* **2014**, *2*, 31.
[48] H. S. Lee, H. Phung, D.-H. Lee, U. Kim, C. T. Nguyen, H. Moon, J. C. Koo, J.-D Nam, H. R. Choi, *Sens. Actuators, A* **2014**, *205*, 191.
[49] H. Boys, G. Frediani, S. Poslad, J. Busfield, F. Carpi, in *Proceedings of SPIE* (Ed: Y. Bar-Cohen), SPIE, Bellingham, WA **2017**, pp. 451–462.
[50] H. Boys, G. Frediani, M. Ghilardi, S. Poslad, J. Busfield, F. Carpi, in *2018 IEEE Int. Conf. on Soft Robotics (RoboSoft)*, IEEE, Philadelphia **2018**, pp. 270–275.
[51] *Ultraleap homepage*, http://leapmotion.com (accessed: February 2021).
[52] J. Guna, G. Jakus, M. Pogačnik, S. Tomažič, J. Sodnik, *Sensors* **2014**, *14*, 3702.
[53] F. Weichert, D. Bachmann, B. Rudak, D. Fisseler, *Sensors* **2013**, *13*, 6380.
[54] L. Maffli, S. Rosset, M. Ghilardi, F. Carpi, H. Shea, *Adv. Funct. Mater.* **2015**, *25*, 1656.
[55] *E. H. Weber on the Tactile Senses*, 2nd ed. (Eds: D. J. Murray, H. E. Ross), Taylor & Francis, London **1996**.
[56] F. B. Madsen, A. E. Daugaard, S. Hvilsted, A. L. Skov, *Macromol. Rapid Commun.* **2016**, *37*, 378.
[57] S. J. Dünki, Y. S. Ko, F. A. Nüesch, D. M. Opris, *Adv. Funct. Mater.* **2015**, *25*, 2467.
[58] A. Poulin, S. Rosset, H. R. Shea, *Appl. Phys. Lett.* **2015**, *107*, 244104.
[59] L. Liu, H. Chen, J. Sheng, J. Zhang, Y. Wang, S. Jia, *Smart Mater. Struct.* **2014**, *23*, 025037.
[60] H. Wang, S. Cai, F. Carpi, Z. Suo, *J. Appl. Mech.* **2012**, *79*, 031008.
[61] D. Xu, A. Tairych, I. Anderson, *Smart Mater. Struct.* **2016**, *25*, 015012.
[62] H. E. Wheat, A. W. Goodwin, A. S. Browning, *J. Neurosci.* **1995**, *15*, 5582.
[63] J. M. Loomis, *Sens. Processes* **1979**, *3*, 289.
[64] S. J. A. Koh, T. Li, J. Zhou, X. Zhao, W. Hong, J. Zhu, Z. Suo, *J. Polym. Sci., Part B: Polym. Phys.* **2011**, *49*, 504.
[65] F. Carpi, I. Anderson, S. Bauer, G. Frediani, G. Gallone, M. Gei, C. Graaf, C. Jean-Mistral, W. Kaal, G. Kofod, M. Kollosche, R. Kornbluh, B. Lassen, M. Matysek, S. Michel, S. Nowak, B. O'Brien, Q. Pei, R. Pelrine, B. Rechenbach, S. Rosset, H. Shea, *Smart Mater. Struct.* **2015**, *24*, 105025.